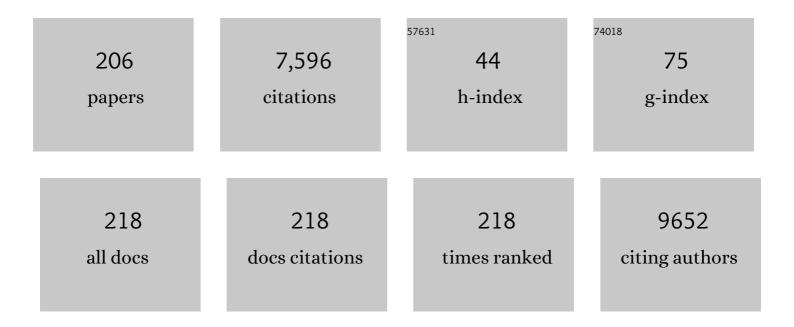
## Chiara Maccato

List of Publications by Year in descending order

Source: https://exaly.com/author-pdf/654775/publications.pdf Version: 2024-02-01



#	Article	IF	CITATIONS
1	Efficient water oxidation at carbon nanotube–polyoxometalate electrocatalytic interfaces. Nature Chemistry, 2010, 2, 826-831.	6.6	459
2	The Potential of Supported Cu <sub>2</sub> O and CuO Nanosystems in Photocatalytic H <sub>2</sub> Production. ChemSusChem, 2009, 2, 230-233.	3.6	225
3	Photocatalytic and antibacterial activity of TiO <sub>2</sub> and Au/TiO <sub>2</sub> nanosystems. Nanotechnology, 2007, 18, 375709.	1.3	197
4	F-Doped Co <sub>3</sub> O <sub>4</sub> Photocatalysts for Sustainable H <sub>2</sub> Generation from Water/Ethanol. Journal of the American Chemical Society, 2011, 133, 19362-19365.	6.6	171
5	1D ZnO nano-assemblies by Plasma-CVD as chemical sensors for flammable and toxic gases. Sensors and Actuators B: Chemical, 2010, 149, 1-7.	4.0	169
6	First Example of ZnOâ^'TiO <sub>2</sub> Nanocomposites by Chemical Vapor Deposition:  Structure, Morphology, Composition, and Gas Sensing Performances. Chemistry of Materials, 2007, 19, 5642-5649.	3.2	164
7	Enhanced Hydrogen Production by Photoreforming of Renewable Oxygenates Through Nanostructured Fe <sub>2</sub> O <sub>3</sub> Polymorphs. Advanced Functional Materials, 2014, 24, 372-378.	7.8	146
8	Co <sub>3</sub> O <sub>4</sub> /ZnO Nanocomposites: From Plasma Synthesis to Gas Sensing Applications. ACS Applied Materials & Interfaces, 2012, 4, 928-934.	4.0	141
9	LaCoO3: Effect of synthesis conditions on properties and reactivity. Applied Catalysis B: Environmental, 2007, 72, 351-362.	10.8	140
10	Novel Synthesis and Gas Sensing Performances of CuO–TiO <sub>2</sub> Nanocomposites Functionalized with Au Nanoparticles. Journal of Physical Chemistry C, 2011, 115, 10510-10517.	1.5	133
11	Supported Metal Oxide Nanosystems for Hydrogen Photogeneration: Quo Vadis?. Advanced Functional Materials, 2011, 21, 2611-2623.	7.8	126
12	Chemical vapor deposition of copper oxide films and entangled quasi-1D nanoarchitectures as innovative gas sensors. Sensors and Actuators B: Chemical, 2009, 141, 270-275.	4.0	114
13	Chiral Strandbergâ€Type Molybdates [(RPO <sub>3</sub> ) <sub>2</sub> Mo <sub>5</sub> O <sub>15</sub> ] <sup>2â^'</sup> as Molecular Gelators: Selfâ€Assembled Fibrillar Nanostructures with Enhanced Optical Activity. Angewandte Chemie - International Edition, 2008, 47, 7275-7279.	7.2	113
14	- International Edition, 2008, 47, 7275-7279. Controlled vapor-phase synthesis of cobalt oxide nanomaterials with tuned composition and spatial organization. CrystEngComm, 2010, 12, 2185.	1.3	110
15	Vertically oriented CuO/ZnO nanorod arrays: from plasma-assisted synthesis to photocatalytic H2 production. Journal of Materials Chemistry, 2012, 22, 11739.	6.7	108
16	Silver nanoparticles deposited on glassy carbon. Electrocatalytic activity for reduction of benzyl chloride. Electrochemistry Communications, 2006, 8, 1707-1712.	2.3	105
17	Fe <sub>2</sub> O <sub>3</sub> –TiO <sub>2</sub> Nanoâ€heterostructure Photoanodes for Highly Efficient Solar Water Oxidation. Advanced Materials Interfaces, 2015, 2, 1500313.	1.9	103
18	Knitting the Catalytic Pattern of Artificial Photosynthesis to a Hybrid Graphene Nanotexture. ACS Nano, 2013, 7, 811-817.	7.3	93

#	Article	IF	CITATIONS
19	Columnar CeO2nanostructures for sensor application. Nanotechnology, 2007, 18, 125502.	1.3	92
20	Molecular Chemisorption on TiO2(110):Â A Local Point of View. Journal of Physical Chemistry B, 1998, 102, 10745-10752.	1.2	91
21	Urchin-like ZnO nanorod arrays for gas sensing applications. CrystEngComm, 2010, 12, 3419.	1.3	90
22	Highly Oriented ZnO Nanorod Arrays by a Novel Plasma Chemical Vapor Deposition Process. Crystal Growth and Design, 2010, 10, 2011-2018.	1.4	89
23	Au/ε-Fe <sub>2</sub> O <sub>3</sub> Nanocomposites as Selective NO <sub>2</sub> Gas Sensors. Journal of Physical Chemistry C, 2014, 118, 11813-11819.	1.5	81
24	Plasma-assisted synthesis of Ag/ZnO nanocomposites: First example of photo-induced H2 production and sensing. International Journal of Hydrogen Energy, 2011, 36, 15527-15537.	3.8	79
25	Vapor Phase Processing of α-Fe <sub>2</sub> O <sub>3</sub> Photoelectrodes for Water Splitting: An Insight into the Structure/Property Interplay. ACS Applied Materials & Interfaces, 2015, 7, 8667-8676.	4.0	76
26	A Pt–Fe Carbon Nitride Nanoâ€electrocatalyst for Polymer Electrolyte Membrane Fuel Cells and Directâ€Methanol Fuel Cells: Synthesis, Characterization, and Electrochemical Studies. Advanced Functional Materials, 2007, 17, 3626-3638.	7.8	73
27	Selective anodes for seawater splitting via functionalization of manganese oxides by a plasma-assisted process. Applied Catalysis B: Environmental, 2021, 284, 119684.	10.8	73
28	CVD of Copper Oxides from a β-Diketonate Diamine Precursor: Tailoring the Nano-Organization. Crystal Growth and Design, 2009, 9, 2470-2480.	1.4	70
29	Electrospun Black Titania Nanofibers: Influence of Hydrogen Plasma-Induced Disorder on the Electronic Structure and Photoelectrochemical Performance. Journal of Physical Chemistry C, 2015, 119, 18835-18842.	1.5	68
30	On the Performances of Cu <sub><i>x</i></sub> O-TiO <sub>2</sub> ( <i>x</i> = 1, 2) Nanomaterials As Innovative Anodes for Thin Film Lithium Batteries. ACS Applied Materials & Interfaces, 2012, 4, 3610-3619.	4.0	64
31	β-Fe <sub>2</sub> O <sub>3</sub> nanomaterials from an iron( <scp>ii</scp> ) diketonate-diamine complex: a study from molecular precursor to growth process. Dalton Transactions, 2012, 41, 149-155.	1.6	63
32	Columnar Fe2O3 arrays via plasma-enhanced growth: Interplay of fluorine substitution and photoelectrochemical properties. International Journal of Hydrogen Energy, 2013, 38, 14189-14199.	3.8	63
33	Rational Design of Ag/TiO <sub>2</sub> Nanosystems by a Combined RFâ€ <del>S</del> puttering/Solâ€Gel Approach. ChemPhysChem, 2009, 10, 3249-3259.	1.0	62
34	Cobalt Oxide Nanomaterials by Vapor-Phase Synthesis for Fast and Reversible Lithium Storage. Journal of Physical Chemistry C, 2010, 114, 10054-10060.	1.5	61
35	Ab Initioand Experimental Studies on the Structure and Relative Stability of thecis-Hydrideâ~η2-Dihydrogen Complexes [{P(CH2CH2PPh2)3}M(H)(I·2-H2)]+(M = Fe, Ru). Inorganic Chemistry, 1997, 36, 1061-1069.	1.9	57
36	Plasma enhanced-CVD of undoped and fluorine-doped Co3O4 nanosystems for novel gas sensors. Sensors and Actuators B: Chemical, 2011, 160, 79-86.	4.0	56

#	Article	IF	CITATIONS
37	CuO/ZnO Nanocomposite Gas Sensors Developed by a Plasmaâ€Assisted Route. ChemPhysChem, 2012, 13, 2342-2348.	1.0	55
38	Gold(III) dithiocarbamate derivatives of N-methylglycine: An experimental and theoretical investigation. Polyhedron, 2005, 24, 521-531.	1.0	54
39	Controlled synthesis and properties of $\hat{l}^2$ -Fe2O3 nanosystems functionalized with Ag or Pt nanoparticles. CrystEngComm, 2012, 14, 6469.	1.3	51
40	An LCAO-LDF study of the chemisorption of H2O and H2S on ZnO(0001) and ZnO(101̄0). Surface Science, 1997, 377-379, 587-591.	0.8	50
41	Photoinduced superhydrophilicity and photocatalytic properties of ZnO nanoplatelets. Surface and Coatings Technology, 2009, 203, 2041-2045.	2.2	50
42	Temperature ontrolled Synthesis and Photocatalytic Performance of ZnO Nanoplatelets. Chemical Vapor Deposition, 2007, 13, 618-625.	1.4	48
43	Ag/ZnO nanomaterials as high performance sensors for flammable and toxic gases. Nanotechnology, 2012, 23, 025502.	1.3	48
44	A Cobalt(II) Hexafluoroacetylacetonate Ethylenediamine Complex As a CVD Molecular Source of Cobalt Oxide Nanostructures. Inorganic Chemistry, 2009, 48, 82-89.	1.9	45
45	Pt-functionalized Fe <sub>2</sub> O <sub>3</sub> photoanodes for solar water splitting: the role of hematite nano-organization and the platinum redox state. Physical Chemistry Chemical Physics, 2015, 17, 12899-12907.	1.3	45
46	Interfacial insight in multi-junction metal oxide photoanodes for water-splitting applications. Nano Energy, 2016, 19, 415-427.	8.2	45
47	A theoretical study of the H2O and H2S chemisorption on Cu2O(111). Applied Surface Science, 1999, 142, 164-168.	3.1	44
48	Luminescent Properties of Eu-Doped Lanthanum Oxyfluoride Solâ^'Gel Thin Films. Journal of Physical Chemistry C, 2009, 113, 14429-14434.	1.5	44
49	Hybrid Polyoxotungstates as Functional Comonomers in New Crossâ€Linked Catalytic Polymers for Sustainable Oxidation with Hydrogen Peroxide. Chemistry - A European Journal, 2012, 18, 13195-13202.	1.7	44
50	Surface Functionalization of Nanostructured Fe <sub>2</sub> O <sub>3</sub> Polymorphs: From Design to Light-Activated Applications. ACS Applied Materials & Interfaces, 2013, 5, 7130-7138.	4.0	44
51	Manufacturing of inorganic nanomaterials: concepts and perspectives. Nanoscale, 2012, 4, 2813.	2.8	43
52	Tailored Vapor-Phase Growth of Cu <sub><i>x</i></sub> O–TiO <sub>2</sub> ( <i>x</i> = 1, 2) Nanomaterials Decorated with Au Particles. Langmuir, 2011, 27, 6409-6417.	1.6	42
53	Supported F-Doped <l>α</l> -Fe <sub>2</sub> O <sub>3</sub> Nanomaterials: Synthesis, Characterization and Photo-Assisted H <sub>2</sub> Production. Journal of Nanoscience and Nanotechnology, 2013, 13, 4962-4968.	0.9	42
54	Multi-component oxide nanosystems by Chemical Vapor Deposition and related routes: challenges and perspectives. CrystEngComm, 2012, 14, 6347.	1.3	41

#	Article	IF	CITATIONS
55	ZnO Nanoplatelets Obtained by Chemical Vapor Deposition, Studied by XPS. Surface Science Spectra, 2007, 14, 19-26.	0.3	40
56	Facile and Reproducible Synthesis of Nanostructured Colloidal ZnO Nanoparticles from Zinc Acetylacetonate: Effect of Experimental Parameters and Mechanistic Investigations. European Journal of Inorganic Chemistry, 2009, 2009, 5017-5028.	1.0	40
57	ZnO Nanorod Arrays by Plasmaâ€Enhanced CVD for Lightâ€Activated Functional Applications. ChemPhysChem, 2010, 11, 2337-2340.	1.0	40
58	Miniemulsions as chemical nanoreactors for the room temperature synthesis of inorganic crystalline nanostructures: ZnO colloids. Journal of Materials Chemistry, 2012, 22, 1620-1626.	6.7	40
59	An iron(II) diamine diketonate molecular complex: Synthesis, characterization and application in the CVD of Fe2O3 thin films. Inorganica Chimica Acta, 2012, 380, 161-166.	1.2	40
60	Solar H2generation via ethanol photoreforming on ε-Fe2O3nanorod arrays activated by Ag and Au nanoparticles. RSC Advances, 2014, 4, 32174.	1.7	40
61	Supported ε and β iron oxide nanomaterials by chemical vapor deposition: structure, morphology and magnetic properties. CrystEngComm, 2013, 15, 1039-1042.	1.3	39
62	Advances in photocatalytic NO <sub>x</sub> abatement through the use of Fe <sub>2</sub> O <sub>3</sub> /TiO <sub>2</sub> nanocomposites. RSC Advances, 2016, 6, 74878-74885.	1.7	39
63	Plasmaâ€Assisted Fabrication of Fe <sub>2</sub> O <sub>3</sub> Co <sub>3</sub> O <sub>4</sub> Nanomaterials as Anodes for Photoelectrochemical Water Splitting. Plasma Processes and Polymers, 2016, 13, 191-200.	1.6	39
64	An Experimental and Theoretical Study of the Electronic Structure of Zinc Thiophenolate-Capped Clusters. Inorganic Chemistry, 1997, 36, 4707-4716.	1.9	37
65	Fe <sub>2</sub> O <sub>3</sub> –TiO <sub>2</sub> nanosystems by a hybrid PE-CVD/ALD approach: controllable synthesis, growth mechanism, and photocatalytic properties. CrystEngComm, 2015, 17, 6219-6226.	1.3	37
66	Vapor Phase Synthesis, Characterization and Gas Sensing Performances of Co <sub>3</sub> O <sub>4</sub> and Au/Co <sub>3</sub> O <sub>4</sub> Nanosystems. Journal of Nanoscience and Nanotechnology, 2010, 10, 8054-8061.	0.9	35
67	Quasi-1D MnO2 nanocomposites as gas sensors for hazardous chemicals. Applied Surface Science, 2020, 512, 145667.	3.1	35
68	Density functional studies of molecular chemisorption on TiO2 (110). Applied Surface Science, 1999, 142, 196-199.	3.1	34
69	TiO2 Thin Films by Chemical Vapor Deposition: An XPS Characterization. Surface Science Spectra, 2007, 14, 27-33.	0.3	34
70	Manganese(II) Molecular Sources for Plasma-Assisted CVD of Mn Oxides and Fluorides: From Precursors to Growth Process. Journal of Physical Chemistry C, 2018, 122, 1367-1375.	1.5	34
71	Toward the Innovative Synthesis of Columnar CeO2Nanostructures. Langmuir, 2006, 22, 8639-8641.	1.6	33
72	Molecular Engineering of Mn <sup>II</sup> Diamine Diketonate Precursors for the Vapor Deposition of Manganese Oxide Nanostructures. Chemistry - A European Journal, 2017, 23, 17954-17963.	1.7	33

#	Article	IF	CITATIONS
73	A comparative study of CO and NO chemisorption on Cu2O(111) and Ag2O(111) non-polar surfaces. Chemical Physics Letters, 1997, 280, 53-58.	1.2	32
74	Straightforward Synthesis of Gold Nanoparticles Supported on Commercial Silica-Polyethyleneimine Beads. Journal of Physical Chemistry C, 2012, 116, 25434-25443.	1.5	32
75	Intrinsic Nitrogenâ€doped CVDâ€grown TiO <sub>2</sub> Thin Films from Allâ€N oordinated Ti Precursors for Photoelectrochemical Applications. Chemical Vapor Deposition, 2013, 19, 45-52.	1.4	32
76	A Comparative Study of CO Chemisorption on Al2O3and Ti2O3Nonpolar Surfaces. Journal of Physical Chemistry B, 2002, 106, 795-802.	1.2	31
77	Pt and Ni Carbon Nitride Electrocatalysts for the Oxygen Reduction Reaction. Journal of the Electrochemical Society, 2007, 154, B745.	1.3	31
78	Vapor Phase Fabrication of Nanoheterostructures Based on ZnO for Photoelectrochemical Water Splitting. Advanced Materials Interfaces, 2017, 4, 1700161.	1.9	30
79	Hematite-based nanocomposites for light-activated applications: Synergistic role of TiO2 and Au introduction. Solar Energy Materials and Solar Cells, 2017, 159, 456-466.	3.0	30
80	Multi-functional MnO <sub>2</sub> nanomaterials for photo-activated applications by a plasma-assisted fabrication route. Nanoscale, 2019, 11, 98-108.	2.8	30
81	CVD Co <sub>3</sub> O <sub>4</sub> Nanopyramids: a Nanoâ€Platform for Photoâ€Assisted H <sub>2</sub> Production. Chemical Vapor Deposition, 2010, 16, 296-300.	1.4	29
82	A plasma-assisted approach for the controlled dispersion of CuO aggregates into β iron( <scp>iii</scp> ) oxide matrices. CrystEngComm, 2014, 16, 8710-8716.	1.3	29
83	Highâ€Performance Olivine for Lithium Batteries: Effects of Ni/Co Doping on the Properties of LiFe <i><sub>α</sub></i> Ni <i><sub>β</sub></i> Co <i><sub>γ</sub></i> PO <sub>4</sub> Cathodes. Advanced Functional Materials, 2015, 25, 4032-4037.	7.8	29
84	SO2 on TiO2(110) and Ti2O3(101̄2) Nonpolar Surfaces:  A DFT Study. Journal of Physical Chemistry B, 2005 109, 12596-12602.	1.2	28
85	Nanostructured iron(III) oxides: From design to gas- and liquid-phase photo-catalytic applications. Thin Solid Films, 2014, 564, 121-127.	0.8	28
86	Toward the Detection of Poisonous Chemicals and Warfare Agents by Functional Mn <sub>3</sub> O <sub>4</sub> Nanosystems. ACS Applied Materials & Interfaces, 2018, 10, 12305-12310.	4.0	28
87	WO <sub>3</sub> -decorated ZnO nanostructures for light-activated applications. CrystEngComm, 2018, 20, 1282-1290.	1.3	28
88	Plasmaâ€Assisted Growth of βâ€MnO <sub>2</sub> Nanosystems as Gas Sensors for Safety and Food Industry Applications. Advanced Materials Interfaces, 2018, 5, 1800792.	1.9	28
89	Reaction of Ketenylidenetriphenylphosphorane (Ph3PCCO) with Platinum(II) and Palladium(II) Complexes. Synthesis, Characterization, and Molecular Structure of [Pt(η3-C3H5){η1-C(PPh3)(CO)}(PPh3)]BF4. Organometallics, 1996, 15, 3250-3252.	1.1	27
90	Organometallic Chemistry of Ph3PCCO. Synthesis, Characterization, X-ray Structure Determination, and Density Functional Study of the First Stable Bis-η1-ketenyl Complex,trans-[PtCl2{η1-C(PPh3)CO}2]. Organometallics, 2000, 19, 1373-1383.	1.1	27

#	Article	IF	CITATIONS
91	MOCVD of ZnO Films from <i>Bis</i> (Ketoiminato)Zn(II) Precursors: Structure, Morphology and Optical Properties. Chemical Vapor Deposition, 2011, 17, 155-161.	1.4	27
92	Plasma Processing of Nanomaterials: Emerging Technologies for Sensing and Energy Applications. Journal of Nanoscience and Nanotechnology, 2011, 11, 8206-8213.	0.9	27
93	Theoretical Investigation of the Chemisorption of H2and CO on the ZnO(101̄0) Surface. Inorganic Chemistry, 1998, 37, 5482-5490.	1.9	26
94	Gas Sensing Properties of Columnar CeO2 Nanostructures Prepared by Chemical Vapor Deposition. Journal of Nanoscience and Nanotechnology, 2008, 8, 1012-1016.	0.9	26
95	Strongly oriented Co3O4 thin films on MgO(100) and MgAl2O4(100) substrates by PE-CVD. CrystEngComm, 2011, 13, 3670.	1.3	26
96	Fluorine doped Fe2O3 nanostructures by a one-pot plasma-assisted strategy. RSC Advances, 2013, 3, 23762.	1.7	26
97	Tailoring Vapor-Phase Fabrication of Mn <sub>3</sub> O <sub>4</sub> Nanosystems: From Synthesis to Gas-Sensing Applications. ACS Applied Nano Materials, 2018, 1, 2962-2970.	2.4	26
98	Sensing Nitrogen Mustard Gas Simulant at the ppb Scale via Selective Dual-Site Activation at Au/Mn <sub>3</sub> O <sub>4</sub> Interfaces. ACS Applied Materials & Interfaces, 2019, 11, 23692-23700.	4.0	26
99	Novel insight into the alignment and structural ordering of supported ZnO nanorods. Chemical Physics Letters, 2010, 500, 287-290.	1.2	25
100	Insights on Growth and Nanoscopic Investigation of Uncommon Iron Oxide Polymorphs. European Journal of Inorganic Chemistry, 2013, 2013, 5454-5461.	1.0	25
101	Theoretical Study of the Chemisorption of CO on Al2O3(0001). Inorganic Chemistry, 2000, 39, 5232-5237.	1.9	24
102	An experimental and theoretical study of the interaction of CH3OH and CH3SH with ZnO. Journal of the Chemical Society, Faraday Transactions, 1996, 92, 3247.	1.7	23
103	A comparative study of the NH3 chemisorption on ZnO(101̄0) and Cu2O(111) non-polar surfaces. Chemical Physics Letters, 1999, 300, 403-408.	1.2	23
104	Organicâ€Inorganic Molecular Nanoâ€5ensors: A Bisâ€Dansylated Tweezerâ€Like Fluoroionophore Integrating a Polyoxometalate Core. European Journal of Organic Chemistry, 2012, 2012, 281-289.	1.2	23
105	Epitaxial-like Growth of Co <sub>3</sub> O <sub>4</sub> /ZnO Quasi-1D Nanocomposites. Crystal Growth and Design, 2012, 12, 5118-5124.	1.4	22
106	Enhancement of Nitrite and Nitrate Electrocatalytic Reduction through the Employment of Self-Assembled Layers of Nickel- and Copper-Substituted Crown-Type Heteropolyanions. Langmuir, 2015, 31, 2584-2592.	1.6	22
107	RF-sputtering preparation of gold-nanoparticle-modified ITO electrodes for electrocatalytic applications. Nanotechnology, 2011, 22, 275711.	1.3	21
108	Vaporâ€Phase Fabrication of βâ€Iron Oxide Nanopyramids for Lithiumâ€Ion Battery Anodes. ChemPhysChem, 2012. 13. 3798-3801.	1.0	21

#	Article	IF	CITATIONS
109	Photoassisted H2 production by metal oxide nanomaterials fabricated through CVD-based approaches. Surface and Coatings Technology, 2013, 230, 219-227.	2.2	21
110	Interplay of thickness and photoelectrochemical properties in nanostructured α-Fe <sub>2</sub> O <sub>3</sub> thin films. Physica Status Solidi (A) Applications and Materials Science, 2015, 212, 1501-1507.	0.8	21
111	Electronic structure of Nb impurities in and on TiO2. Physical Chemistry Chemical Physics, 1999, 1, 3793-3799.	1.3	20
112	An old workhorse for new applications: Fe(dpm) <sub>3</sub> as a precursor for low-temperature PECVD of iron( <scp>iii</scp> ) oxide. Physical Chemistry Chemical Physics, 2015, 17, 11174-11181.	1.3	20
113	Synthesis and conformational characterization of functional di-block copolymer brushes for microarray technology. Applied Surface Science, 2012, 258, 3750-3756.	3.1	19
114	Nitrate and Nitrite Electrocatalytic Reduction at Layer-by-Layer Films Composed of Dawson-type Heteropolyanions Mono-substituted with Transitional Metal Ions and Silver Nanoparticles. Electrochimica Acta, 2015, 184, 323-330.	2.6	18
115	Iron–Titanium Oxide Nanocomposites Functionalized with Gold Particles: From Design to Solar Hydrogen Production. Advanced Materials Interfaces, 2016, 3, 1600348.	1.9	18
116	Engineering Au/MnO <sub>2</sub> hierarchical nanoarchitectures for ethanol electrochemical valorization. Journal of Materials Chemistry A, 2020, 8, 16902-16907.	5.2	18
117	Doping of TiO <sub>2</sub> as a tool to optimize the water splitting efficiencies of titania–hematite photoanodes. Sustainable Energy and Fuels, 2017, 1, 199-206.	2.5	17
118	Copper Vanadate Nanobelts as Anodes for Photoelectrochemical Water Splitting: Influence of CoO <i><sub>x</sub></i> Overlayers on Functional Performances. ACS Applied Materials & Interfaces, 2020, 12, 31448-31458.	4.0	17
119	A theoretical investigation of BrÃ,nsted acids chemisorption on ZnO(0001). Surface Science, 1995, 343, 115-132.	0.8	16
120	Experimental and Theoretical Investigation of the Molecular and Electronic Structure of [Zn4(μ4-S){μ-S2As(CH3)2}6] and [Cd4(μ4-S){μ-S2As(CH3)2}6]: Two Possible Molecular Models of Exten Metal Chalcogenide Semiconductorsâ€. Inorganic Chemistry, 1999, 38, 1145-1152.	deda	16
121	Ag and Pt Particles Sputtered on β-Fe2O3: An XPS Investigation. Surface Science Spectra, 2012, 19, 1-12.	0.3	16
122	Structure and properties of Mn3O4 thin films grown on single crystal substrates by chemical vapor deposition. Materials Chemistry and Physics, 2019, 223, 591-596.	2.0	16
123	Enhanced photocatalytic removal of NOx gases by β-Fe2O3/CuO and β-Fe2O3/WO3 nanoheterostructures. Chemical Engineering Journal, 2022, 430, 132757.	6.6	16
124	A theoretical investigation of the relaxation effects induced on the ZnO(101Ì,,0) surface by the chemisorption of H2 and CO. Applied Surface Science, 1999, 142, 192-195.	3.1	15
125	Effect of microwave assisted and conventional thermal heating on the evolution of nanostructured inorganic–organic hybrid materials to binary ZrO2–SiO2 oxides. Journal of Materials Chemistry, 2007, 17, 4387.	6.7	15
126	Controllable vapor phase fabrication of F:Mn <sub>3</sub> O <sub>4</sub> thin films functionalized with Ag and TiO <sub>2</sub> . CrystEngComm, 2018, 20, 3016-3024.	1.3	15

#	Article	IF	CITATIONS
127	Controlled Surface Modification of ZnO Nanostructures with Amorphous TiO <sub>2</sub> for Photoelectrochemical Water Splitting. Advanced Sustainable Systems, 2019, 3, 1900046.	2.7	15
128	Manganese Oxide Nanoarchitectures as Chemoresistive Gas Sensors to Monitor Fruit Ripening. Journal of Nanoscience and Nanotechnology, 2020, 20, 3025-3030.	0.9	15
129	Mild fabrication of silica-silver nanocomposites as active platforms for environmental remediation. RSC Advances, 2015, 5, 9600-9606.	1.7	14
130	Hydrogen Gas Sensing Performances of p-Type Mn3O4 Nanosystems: The Role of Built-in Mn3O4/Ag and Mn3O4/SnO2 Junctions. Nanomaterials, 2020, 10, 511.	1.9	14
131	Metal Oxide Nanosystems As Chemoresistive Gas Sensors for Chemical Warfare Agents: A Focused Review. Advanced Materials Interfaces, 2022, 9, .	1.9	14
132	A soft Plasma Enhanced-Chemical Vapor Deposition process for the tailored synthesis of SiO2 films. Thin Solid Films, 2008, 516, 7393-7399.	0.8	13
133	Multi-Functional Copper Oxide Nanosystems for H2 Sustainable Production and Sensing. ECS Transactions, 2009, 25, 1169-1176.	0.3	13
134	Fluoroalkylsilanes with Embedded Functional Groups as Building Blocks for Environmentally Safer Self-Assembled Monolayers. Langmuir, 2015, 31, 6988-6994.	1.6	13
135	Supported Mn <sub>3</sub> O <sub>4</sub> Nanosystems for Hydrogen Production through Ethanol Photoreforming. Langmuir, 2018, 34, 4568-4574.	1.6	13
136	Tracking Fluorescent Polyoxometalates within Cells. European Journal of Inorganic Chemistry, 2018, 2018, 4955-4961.	1.0	13
137	Multilayer assemblies of a Cu-phthalocyanine with Dawson type polyoxometalates (POMs) for the electrocatalytic reduction of phosphate. Journal of Electroanalytical Chemistry, 2020, 858, 113770.	1.9	13
138	Cerium (III) Fluoride Thin Films by XPS. Surface Science Spectra, 2006, 13, 87-93.	0.3	12
139	Silica-sandwiched Au nanoparticle arrays by a soft PE-CVD/RF sputtering approach. Nanotechnology, 2008, 19, 255602.	1.3	12
140	Tailoring iron( <scp>III</scp> ) oxide nanomorphology by chemical vapor deposition: Growth and characterization. Physica Status Solidi (A) Applications and Materials Science, 2014, 211, 316-322.	0.8	12
141	PECVD of <i>Hematite</i> Nanoblades and Nanocolumns: Synthesis, Characterization, and Growth Model. Chemical Vapor Deposition, 2015, 21, 294-299.	1.4	12
142	Novel two-step vapor-phase synthesis of UV–Vis light active Fe2O3/WO3 nanocomposites for phenol degradation. Environmental Science and Pollution Research, 2016, 23, 20350-20359.	2.7	12
143	XPS investigation of F-doped MnO2 nanosystems fabricated by plasma assisted-CVD. Surface Science Spectra, 2018, 25, .	0.3	12
144	Mn3O4 thin films functionalized with Ag, Au, and TiO2 analyzed using x-ray photoelectron spectroscopy. Surface Science Spectra, 2018, 25, 014003.	0.3	12

#	Article	IF	CITATIONS
145	Mn <sub>3</sub> O <sub>4</sub> Nanomaterials Functionalized with Fe <sub>2</sub> O <sub>3</sub> and ZnO: Fabrication, Characterization, and Ammonia Sensing Properties. Advanced Materials Interfaces, 2019, 6, 1901239.	1.9	12
146	Quasi-1D Mn <sub>2</sub> O <sub>3</sub> Nanostructures Functionalized with First-Row Transition-Metal Oxides as Oxygen Evolution Catalysts. ACS Applied Nano Materials, 2020, 3, 9889-9898.	2.4	12
147	Plasmaâ€Assisted Synthesis of Co <sub>3</sub> O <sub>4</sub> â€Based Electrocatalysts on Ni Foam Substrates for the Oxygen Evolution Reaction. Advanced Materials Interfaces, 2021, 8, 2100763.	1.9	12
148	Tailoring oxygen evolution performances of carbon nitride systems fabricated by electrophoresis through Ag and Au plasma functionalization. Chemical Engineering Journal, 2022, 448, 137645.	6.6	12
149	Proteins conjugation with ZnO sol–gel nanopowders. Journal of Sol-Gel Science and Technology, 2011, 60, 352-358.	1.1	11
150	Surface Decoration of <i>ïµ</i> â€Fe <sub>2</sub> O <sub>3</sub> Nanorods by CuO Via a Two‣tep CVD/Sputtering Approach <b>**</b> . Chemical Vapor Deposition, 2014, 20, 313-319.	1.4	11
151	Hydrogen peroxide activation by fluorophilic polyoxotungstates for fast and selective oxygen transfer catalysis. Dalton Transactions, 2016, 45, 14544-14548.	1.6	11
152	Innovative M(Hfa)2•TMEDA (M=Cu, Co) Precursors for the CVD of Copper-Cobalt Oxides: an Integrated Theoretical and Experimental Approach. ECS Transactions, 2009, 25, 549-556.	0.3	10
153	Fluorine-Doped Iron Oxide Nanomaterials by Plasma Enhanced-CVD: An XPS Study. Surface Science Spectra, 2013, 20, 9-16.	0.3	10
154	A study of $Pt\hat{I}$ ±-Fe2O3 Nanocomposites by XPS. Surface Science Spectra, 2015, 22, 47-57.	0.3	10
155	XPS analysis of Fe2O3-TiO2-Au nanocomposites prepared by a plasma-assisted route. Surface Science Spectra, 2016, 23, 61-69.	0.3	10
156	Fe2O3-TiO2 nanocomposites on activated carbon fibers by a plasma-assisted approach. Surface and Coatings Technology, 2016, 307, 352-358.	2.2	10
157	Controlled Growth of Supported ZnO Inverted Nanopyramids with Downward Pointing Tips. Crystal Growth and Design, 2018, 18, 2579-2587.	1.4	10
158	A LCAO-LDF study of Bra^nsted acids chemisorption on ZnO(0001). Surface Science, 1996, 352-354, 341-345.	0.8	9
159	Determination of thermooptical and transport parameters of ε iron(III) oxide-based nanocomposites by beam deflection spectroscopy. Optical Materials, 2015, 42, 370-375.	1.7	9
160	Insights into the Plasma-Assisted Fabrication and Nanoscopic Investigation of Tailored MnO <sub>2</sub> Nanomaterials. Inorganic Chemistry, 2018, 57, 14564-14573.	1.9	9
161	Electrochemical, surface and electrocatalytic properties of layer-by-layer multilayer assemblies composed of silver nanoparticles and a Ni(II)-crown type polyoxometalate. Journal of Electroanalytical Chemistry, 2018, 824, 75-82.	1.9	9
162	High Magnetic Coercivity in Nanostructured Mn3O4 Thin Films Obtained by Chemical Vapor Deposition. ACS Applied Nano Materials, 2019, 2, 1704-1712.	2.4	9

#	Article	IF	CITATIONS
163	Facile preparation of a cobalt diamine diketonate adduct as a potential vapor phase precursor for Co <sub>3</sub> O <sub>4</sub> films. Dalton Transactions, 2021, 50, 10374-10385.	1.6	9
164	The Early Steps of Molecule-to-Material Conversion in Chemical Vapor Deposition (CVD): A Case Study. Molecules, 2021, 26, 1988.	1.7	9
165	LCAO-LDA Study of the chemisorption of formate on Cu(110) and Ag(110) surfaces. Journal of the Chemical Society, Faraday Transactions, 1998, 94, 797-804.	1.7	8
166	An experimental and theoretical study of the electronic and molecular structure of [Zn4(?4-S){μ-S2P(OC2H5)2}6]: the first molecular model of ZnS. Journal of Organometallic Chemistry, 2000, 593-594, 307-314.	0.8	8
167	A Comparative Theoretical Investigation of Three Sodalite Systems:Â Cd4S(AlO2)6, Zn4O(BO2)6, and Zn4S(BO2)6. Journal of Physical Chemistry B, 2002, 106, 2569-2573.	1.2	8
168	Low-Temperature PECVD of Transparent SiOxCyHz Thin Films. Chemical Vapor Deposition, 2007, 13, 205-210.	1.4	8
169	On the use of Fe(dpm) <sub>3</sub> as precursor for the thermal VD growth of <i>hematite</i> nanostructures. Physica Status Solidi (A) Applications and Materials Science, 2017, 214, 1600779.	0.8	8
170	Magnetic properties of ε iron(III) oxide nanorod arrays functionalized with gold and copper(II) oxide. Applied Surface Science, 2018, 427, 890-896.	3.1	8
171	XPS characterization of Mn2O3 nanomaterials functionalized with Ag and SnO2. Surface Science Spectra, 2020, 27, .	0.3	8
172	Rational synthesis of F-doped iron oxides on Al2O3(0001) single crystals. RSC Advances, 2014, 4, 52140-52146.	1.7	7
173	TiO2-Fe2O3 and Co3O4-Fe2O3 nanocomposites analyzed by X-ray Photoelectron Spectroscopy. Surface Science Spectra, 2015, 22, 34-46.	0.3	7
174	MOCVD of TiO <sub>2</sub> thin films from a modified titanium alkoxide precursor. Physica Status Solidi (A) Applications and Materials Science, 2015, 212, 1563-1570.	0.8	7
175	Surface Functionalization of Grown-on-Tip ZnO Nanopyramids: From Fabrication to Light-Triggered Applications. ACS Applied Materials & amp; Interfaces, 2019, 11, 15881-15890.	4.0	7
176	Tailored Co <sub>3</sub> O <sub>4</sub> -Based Nanosystems: Toward Photocatalysts for Air Purification. ACS Applied Materials & Interfaces, 2021, 13, 44520-44530.	4.0	7
177	A versatile Fe(II) diketonate diamine adduct: Preparation, characterization and validation in the chemical vapor deposition of iron oxide nanomaterials. Materials Chemistry and Physics, 2022, 277, 125534.	2.0	7
178	Fe2O3-CuO Nanocomposites Prepared by a Two-step Vapor Phase Strategy and Analyzed by XPS. Surface Science Spectra, 2014, 21, 1-9.	0.3	6
179	Nanoscale Mn <sub>3</sub> O <sub>4</sub> Thin Film Photoelectrodes Fabricated by a Vapor-Phase Route. ACS Applied Energy Materials, 2019, 2, 8294-8302.	2.5	6
180	MnO2 nanomaterials functionalized with Ag and SnO2: An XPS study. Surface Science Spectra, 2020, 27, 024005.	0.3	6

#	Article	IF	CITATIONS
181	Alkyl chain grafting on silica–zirconia mixed oxides: preparation and characterization. Journal of Materials Chemistry, 2010, 20, 2345.	6.7	5
182	Fe 2 O 3 nanostructures on SrTiO 3 (1 1 1) by chemical vapor deposition: Growth and characterization. Materials Letters, 2014, 136, 141-145.	1.3	5
183	Au–Manganese Oxide Nanostructures by a Plasmaâ€Assisted Process as Electrocatalysts for Oxygen Evolution: A Chemicoâ€Physical Investigation. Advanced Sustainable Systems, 2020, , 2000177.	2.7	5
184	Plasma-Assisted Chemical Vapor Deposition of F-Doped MnO2 Nanostructures on Single Crystal Substrates. Nanomaterials, 2020, 10, 1335.	1.9	5
185	Dual Improvement of <i>β</i> â€MnO <sub>2</sub> Oxygen Evolution Electrocatalysts via Combined Substrate Control and Surface Engineering. ChemCatChem, 2020, 12, 5984-5992.	1.8	5
186	Layer-by-layer assembly of graphene oxide and 12-molybdosilicate composite films for the electrocatalytic reduction of chloroform in neutral aqueous solution. Electrochimica Acta, 2020, 343, 135987.	2.6	5
187	A Cu( <scp>ii</scp> )-MOF based on a propargyl carbamate-functionalized isophthalate ligand. RSC Advances, 2021, 11, 20429-20438.	1.7	5
188	Viral Nanotemplates Armed with Oxygenic Polyoxometalates for Hydrogen Peroxide Detoxification. European Journal of Inorganic Chemistry, 2015, 2015, 3457-3461.	1.0	4
189	Fe2O3-WO3 nanosystems synthesized by a hybrid CVD/sputtering route, and analyzed by X-ray photoelectron spectroscopy. Surface Science Spectra, 2016, 23, 93-101.	0.3	4
190	Gold nanoparticles-decorated fluoroalkylsilane nano-assemblies for electrocatalytic applications. Applied Surface Science, 2016, 362, 42-48.	3.1	4
191	Tailored Fabrication of Transferable and Hollow Weblike Titanium Dioxide Structures. ChemPhysChem, 2017, 18, 64-71.	1.0	4
192	Metal oxide electrodes for photo-activated water splitting. , 2018, , 19-48.		4
193	Chemical Vapor Deposition of Cu <inf>2</inf> O and CuO nanosystems for innovative gas sensors. , 2009, , .		3
194	Self-Cleaning and Anti-Fogging Surfaces Based on Nanostructured Metal Oxides. Advances in Science and Technology, 2014, 91, 39-47.	0.2	3
195	ZnO-based nanocomposites prepared by a vapor phase route, investigated by XPS. Surface Science Spectra, 2018, 25, .	0.3	3
196	Analysis of Co3O4-SnO2 and Co3O4-Fe2O3 nanosystems by x-ray photoelectron spectroscopy. Surface Science Spectra, 2021, 28, 024002.	0.3	3
197	Zinc and Copper Oxides Functionalized with Metal Nanoparticles: An Insight Into Their Nano-Organization. Journal of Advanced Microscopy Research, 2012, 7, 84-90.	0.3	2
198	Fe2O3-WO3 and Fe2O3-CuO nanoheterostructures by XPS. Surface Science Spectra, 2021, 28, .	0.3	2

#	Article	IF	CITATIONS
199	Surface-Driven Porphyrin Self-Assembly on Pre-Activated Si Substrates. Journal of Nanoscience and Nanotechnology, 2011, 11, 3235-3244.	0.9	1
200	Hydrogen Photogeneration: Supported Metal Oxide Nanosystems for Hydrogen Photogeneration: Quo Vadis? (Adv. Funct. Mater. 14/2011). Advanced Functional Materials, 2011, 21, 2610-2610.	7.8	1
201	Erratum to "An experiment and theoretical study of the electronic and molecular structure of [Zn4(μ4-S){μ-S2P(OC2H5)2}6]: the first molecular model of ZnS― Journal of Organometallic Chemistry, 2000, 601, 343.	0.8	0
202	Silica-Based Thin Films by PE-CVD: An XPS Characterization. Surface Science Spectra, 2006, 13, 81-86.	0.3	0
203	Gold nanoparticles as markers for fluorinated surfaces containing embedded amide groups. Applied Surface Science, 2018, 440, 1235-1243.	3.1	0
204	Chemical Vapor Deposition: Mn <sub>3</sub> O <sub>4</sub> Nanomaterials Functionalized with Fe <sub>2</sub> O <sub>3</sub> and ZnO: Fabrication, Characterization, and Ammonia Sensing Properties (Adv. Mater. Interfaces 24/2019). Advanced Materials Interfaces, 2019, 6, 1970151.	1.9	0
205	Plasmaâ€Assisted Synthesis of Co <sub>3</sub> O <sub>4</sub> â€Based Electrocatalysts on Ni Foam Substrates for the Oxygen Evolution Reaction (Adv. Mater. Interfaces 18/2021). Advanced Materials Interfaces, 2021, 8, 2170099.	1.9	0
206	Fabrication and Characterization of Fe <sub>2</sub> O <sub>3</sub> -Based Nanostructures Functionalized with Metal Particles and Oxide Overlayers. Journal of Advanced Microscopy Research, 2015, 10, 239-243.	0.3	0